View metadata, citation and similar papers at core.ac.uk
brought to you by CORE
provided by CorpusUL

Optical emission spectroscopy as a process-monitoring tool in plasma enhanced chemical vapor deposition of amorphous carbon coatings - multivariate statistical modelling

LABORATOIRE LIS
D'INGÉNIERIE DE SURFACE

Farid Anooshehpour[1,2,3], Stéphane Turgeon[1,2,3], Maxime Cloutier[1,3], Diego Mantovani[1,3], and Gaétan Laroche[2,3]

1Laboratory for Biomaterials and Bioengineering, Canada Research Chair Tier I in Biomaterials and Bioengineering for the Innovation in Surgery, Department of Mining, Metallurgy and Materials Engineering, CHU de Québec Research Center, Université Laval, 1065 Medicine Street, G1V 0A6 Québec, Canada
[2]Laboratoire d'Ingénierie de Surface, Centre de Recherche sur les Matériaux Avancés, Département de génie des mines, de la métallurgie et des matériaux, Université Laval 1045 avenue de la Médecine, Bureau 1033, Québec, G1V 0A6 Québec, Canada
[3]Centre de recherche du CHU de Québec, Hôpital St-François d'Assise, 10 rue de l'Espinay, Québec, G1L 3L5, Québec, Canada.

ABSTRACT
Production of Diamond-Like Carbon (DLC) nanocoatings using plasma enhanced chemical vapor deposition is studied by Optical Emission Spectroscopy (OES) as a plasma diagnostic technique. The objective of the current research is to establish a predictive model of DLC properties using a multivariate analysis method. This model is based on OES data instead of process parameters, which are reactor dependent and accordingly, their effect on the plasma deposition process may vary from one reactor to another. The predictive potential of OES is evaluated using partial least square regression (PLSR) analysis. The results show that OES derived data are capable of replacing some process parameters to predict the DLC properties. The perspective of PLSR modelling and OES application for the development and monitoring of a structurally graded DLC coating is also discussed.

KEYWORDS
Diamond-like coating, Plasma characterization, Surface characterization, Partial least square regression

CITATION
Anooshehpour, F., Turgeon, S., Cloutier, M., Mantovani, D., & Laroche, G. (2018). Optical emission spectroscopy as a process-monitoring tool in plasma enhanced chemical vapor deposition of amorphous carbon coatings-multivariate statistical modelling. Thin Solid Films, 649, 106-114.

This is the author's version of the original manuscript. The final publication is available at Elsevier Link Online via https://doi.org/10.1016/j.tsf.2018.01.029

1 INTRODUCTION

Diamond Like Carbon (DLC) is a general term that covers a wide range of amorphous carbon materials including amorphous carbon (a-C, a mix of sp^2 and sp^3 hybridized carbon), tetrahedral amorphous carbon (ta-C) with up to 90% of carbon in sp3 hybridization (diamond-like structure) and their hydrogenated variants (a-C:H and ta-C:H) [1–3]. Therefore, the sp^3/sp^2 ratio and H-content determine the final DLC structure and properties. However, a high sp^3 content of a DLC coating

provokes a high internal compressive stress within the coating, which restricts film thickness and its application in harsh conditions. Annealing [4,5], doping with different types of metallic elements [6–8] and multi-layer or structurally graded DLC [9–11] have been proposed to attenuate the internal stress and to improve the coating's mechanical behavior. The latter has the benefit of tailoring the properties of the coating according to the desired application.

Designing a graded coating requires to know the correlation between the structure of nanocoating and the plasma process parameters. Several researchers have studied the effects of process parameters such as plasma power, pressure, etc. on the properties of DLC coatings [12,13]. However, the relationship between such parameters and plasma characteristics, which directly affect a coating's structure, differs from one reactor to another depending on each reactor's configuration. Consequently, reproducing identical coatings in different plasma setups involves a tedious trial and error procedure. One avenue to overcome this problem consists in correlating some of the plasma characteristics in terms of plasma specie densities and energies, as measured through plasma diagnostic tools, with the DLC coating properties.

Several plasma diagnostic methods have been used to study carbon containing plasmas; such as electrostatic probes [14–16], optical emission spectroscopy (OES), optical absorption spectroscopy [17–20], and mass spectroscopy [21–23]. Each of these plasma characterization methods has pros and cons. For instance, the Langmuir probe is a common method for evaluating electron energy distribution inside the plasma. However, it is an intrusive characterization method, which means that it somewhat perturbs the plasma environment. On the other hand, OES extrinsically probes the plasma and provides information about temperatures (electronic, vibrational, and/or rotational) and densities of excited species. Although being advantageous at first sight, this technique requires to make some hypotheses related to the energy distribution of the plasma species as well as the mechanisms of excitation [24,25].

In this context, this article aims to compare both the deposition process parameters and OES data as predictive tools to monitor DLC structure and its mechanical properties. However, since the plasma parameters, optical spectroscopy results, and coating properties are highly correlated, the common regression methods cannot demonstrate the effects of each independent parameter on the resulting dependent variables. Therefore, a partial least square (PLS) regression modeling, which is consistent with effects causing changes in the investigated system [26], is employed to find the correlation between either the plasma process parameters or OES data with some of the DLC structural and mechanical properties.

1.1 Statistical analysis—PLSR

Projection to Latent Structure/Partial Least Square Regression (PLSR) is a practical mathematical tool to study a data space when numerous, correlated, noisy and sometimes missing data are available. It extracts the latent structure of independent (X) and dependent (Y) data set by finding new coordinate system for X and Y based on orthogonal vectors (called Principal Components (PC) or Latent Variables) along which there is minimum variance between the projected observations. The PCs are the best descriptors of each data space (X or Y). This new coordinate system is calculated in such a way that it assures the highest possible covariance between X and Y spaces. Therefore, a PLSR model describes at the same time the data structure at predictive (X) and predicted (Y) matrices as well as the correlation between these two [26].

A PLS model begins by following decompositions of X and Y matrices [26] (when there are N observations with K variables in X and M responses in Y):

$$X_{NxK} = T_{NxK} + P_{AxK}^{T} + E_{NxK} \quad (1)$$

$$Y_{NxM} = U_{NxA}C_{AxM}^{T} + F_{NxM} \quad (2)$$

$$T_{NxA} = X_{NxK}W_{KxA}^{*} \quad (3)$$

T and U are called score matrices for X and Y, respectively, and bear the A principal components of the X and Y matrices in their columns. P and C are called loading matrices. E and F are the residuals of the model for X and Y, respectively. W* is called the weight matrix of PLSR and contains those combinations of X variables that are the most predictive of Y.

In PLSR, the T and U matrices are calculated in such a way that a high level of correlation between them is assured. Therefore, T is also a good predictor of Y:

$$Y_{NxM} = T_{NxA}C_{AxM}^{T} + G_{NxM} \quad (4)$$

A combination of Eqs. (3)-(5) will be used for the purpose of process prediction:

$$Y_{NxM} = X_{NxK}W_{KxA}^{*}C_{AxM}^{T} + G_{NxM} = X_{NxK}B_{KxM} + G_{NxM} \quad (5)$$

This last equation allows to determine the B matrix that contains the regression coefficients. More details on PLSR is provided by Wold [26].

2 MATERIALS AND METHODS

Amorphous carbon films were deposited using an inductively coupled radio frequency plasma enhanced chemical vapor deposition (RF-PECVD) reactor (FLR1200, Plasmionique Inc., Varennes, QC, Canada) over silicon wafers. Figure 1 depicts a schematic setup of the plasma reactor. Methane (CH_4) was used as the source of carbon and hydrogen. A separate low frequency power supply was employed to induce ion acceleration toward substrates by applying a self-rectified negative bias voltage to the sample holder (as a cathode) with respect to the chamber wall (as the Anode). A UV-Vis spectrometer equipped with a 300 lines per mm grating (HR4000CG-UV-NIR, Ocean Optics Inc. Dunedin, FL, USA) was used to record the UV-Visible spectra between 200 and 1100 nm with a spectral resolution of ~ 0.5 nm.

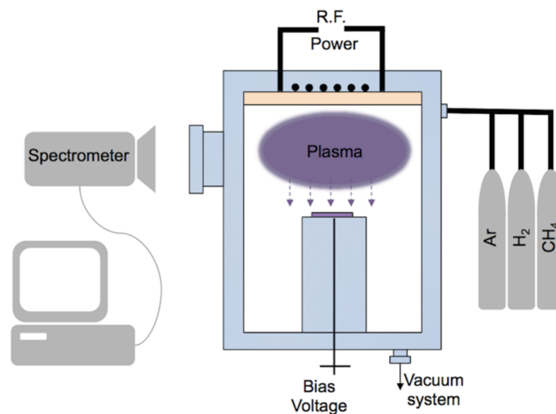

Figure 1. Schematic set up of the PECVD reactor used in this work.

2.1 Pre-deposition process

Silicon substrates were wiped with acetone and then fixed over the substrate holder in such a way to ensure proper electrical conductivity between the substrate holder disk and samples during the deposition process. Argon etching (at 100 W, 20 sccm, 6.7 Pa, and a bias voltage of -100 V for 15 min) for contamination removal and hydrogen etching (at 100 W, 10 sccm, 6.7 Pa, and a bias voltage of -150 V for 15 min) for surface activation were carried out prior to deposition

2.2 DLC deposition

A constant flow of 7 sccm of CH_4 provided the required carbon source to build-up the diamond-like coating during 30 min of deposition. Four experimental parameters were studied in this research; plasma RF power (P), plasma power mode (M) (either continuous or pulse mode at 100Hz and duty cycle of 50%), pressure (p), and applied bias voltage (V_b).

2.2.1 Determination of deposition parameters

The four experimental parameters mentioned above were employed at two different levels (high/low), as described in Table 1. This range of values allowed the deposition of DLC coatings with a variety of structural and mechanical properties.

Table 1: Range of experimental parameters used for DLC deposition.

	Plasma Power	Plasma mode	Pressure	Bias voltage
Unit	[W]	-	[Pa]	[V]
Label	P	M	p	V_b
Low (-)	100	0 for Continuous	1.3	-50
High (+)	300	1 for Pulse (at 100 Hz freq.)	4.0	-200

2.2.2 Design of experiments

A fractional factorial design method was employed to determine the combination of experimental parameters for each deposition condition and to reduce the number of experiments [27]. Therefore, 8 observations (Table 2) with 3 replicates were performed. This allowed to build-up the training set of experiments that will be used to develop the statistical model.

The range of values has been determined based on literature [27], technical limitations, and a series of preliminary tests. For example, at a bias voltage of less than 50 V, the incident carbon species do not carry enough energy to form a dense sp^3 structure over the substrate. Therefore, the resulting coating would not be stable. However, when they got accelerated at very high bias voltage (over 200 V), they induce intolerable internal stresses to the coating that make it delaminated.

The lower value for the pressure and plasma power are the minimum values which are capable of igniting and keeping a steady state plasma medium, according to our experimental setup. Their high values are determined based on our experimental setup limitations.

Supplementary sets of coatings were also deposited for evaluation of the model prediction power (prediction set). As may be seen in Table 2, the combinations of experimental parameters for the prediction set were different from those of the training set.

Table 2. Combination of experimental parameters and the resulted coating properties and collected OES data for the Training and the Prediction sets of experiments. The errors represent the standard deviation of at least 3 measurements for each specific parameter.

	Experimental data					OES data				Coating properties		
	Test ID	P	V	M	p	CH/Ar	H_α /Ar	H_β/Ar	FWHM-H_α (nm)	Deposition rate (nm)	Internal Stress (GPa)	D value (eV)
Training Set	A	+	+	+	+	1.2±0.2	35±1	6±1				
	B	+	+	-	-	1.28±0.01	10.4±0.3	6.4±0.4				
	C	+	-	+	+	1.2±0.1	35±1	6±1	1.2±0.2	9.8	0.06±0.02	16±1
	D	+	-	-	-	1.26±0.01	-	6.73±0.02	1.15	8±2	0.08±0.02	14.4±0.3
	E	-	+	+	-	1.79±0.04	6.7±0.1	1.6±0.1	1.14±0.05	3.0±0.2	2.9±0.4	13.7±0.5
	F	-	+	-	+	1.0±0.1	19±3	2.8±0.5	1.13±0.02	3.0±0.4	2.0±0.3	14.05±0.09
	G	-	-	+	-	1.60±0.05	11±1	2.3±0.8	1.10±0.09	6.0±0.2	0.49±0.03	14.1±0.1
	H	-	-	-	+	0.93±0.02	17±2	2.5±0.2	1.13±0.04	3.8±0.4	0.5±0.1	14.3±0.4
Prediction set	P1	-	-	+	+	1.3±0.5	16±5	2.3±0.4	1.07±0.03	3.5±0.5	0.29±0.01	14.4±0.4
	P2	-	+	+	+	1.15±0.01	1.88±0.05	1.19±0.08	1.06±0.05	2.7±0.3	2.8±0.4	13.4±0.2
	P3	+	-	+	-	1.23±0.01	19±3	8.04±0.02	2.60±0.08	5.3±0.2	0.16±0.05	14.8±0.2
	P4	-	+	-	-	1.28±0.01	2.31±0.06	1.17±0.07	1.18±0.05	3.0±0.3	0.90±0.03	13.5±0.3

2.3 DLC characterization methods

2.3.1 Profilometry

The thickness of coatings was measured using a stylus profilometer (DektakXT, Bruker, USA) with a force of 3 mg applied to a 12.5 μm R_c stylus via a step-height technique. The internal compressive stress was calculated by measuring the surface curvature before and after deposition using the same surface profilometer and the Stoney's method [28].

2.3.2 Profilometry X-ray Auger electron spectroscopy (XAES)

The structure of DLC was studied by XAES [29,30]. The D-parameter, which is the energy difference between the highest peak and the lowest valley in the first derivative of the C KLL Auger peak, is related to sp^3/sp^2 ratio and its values range from about 24 eV for graphite to 14 eV for a perfect diamond structure [29,31,32]. The XAES analysis was carried out from the Auger signal measured using a PHI 5600-ci XPS spectrometer with an Al-standard anode in the pseudo-bonding energy range of 1200-1250 eV (Physical Electronics USA, Chanhassen, MN). An example of the calculation of this parameter from the XAES data is provided in Figure 2.

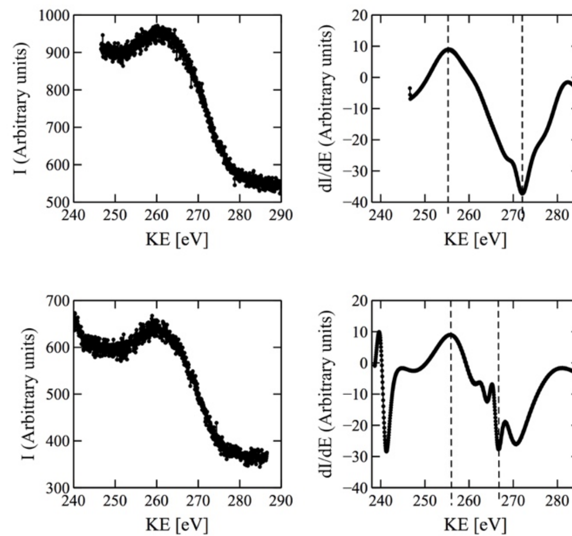

Figure 2. C KLL peaks (left) and their first derivative (right) for two samples with low and high D values.

2.4 Plasma diagnostics (OES)

There are numerous studies on optical spectroscopy of carbon containing plasmas used either for carbon nanotube production or amorphous carbon coating deposition [17,33–36]. The knowledge gained from these publications enables the use of OES as a tool to control the process of DLC coating through PECVD. Depending on precursor gas composition and plasma conditions, different spectral lines could be observed in an emission spectrum [37–40]. As may be seen in Figure 3, the emission spectrum of the investigated plasma in a methane environment exhibits features which origin from the dissociation of this molecule within the plasma environment. Indeed, Hα and Hβ lines are related to Balmer transitions in hydrogen atoms. In addition, an emission line is assigned to the presence of CH moieties, indicating H removal from CH_4. Finally, the H_2 lines are related to the recombination of two hydrogen atoms within the plasma while the Ar lines come from residual argon used during the etching step. In addition to providing information about the nature of the species, these lines can also be used to calculate their kinetic energies as well as densities in the plasma environment, as described below. Of note, the presence of C_2 lines, although reported by others [17,34], was not observed in the present study.

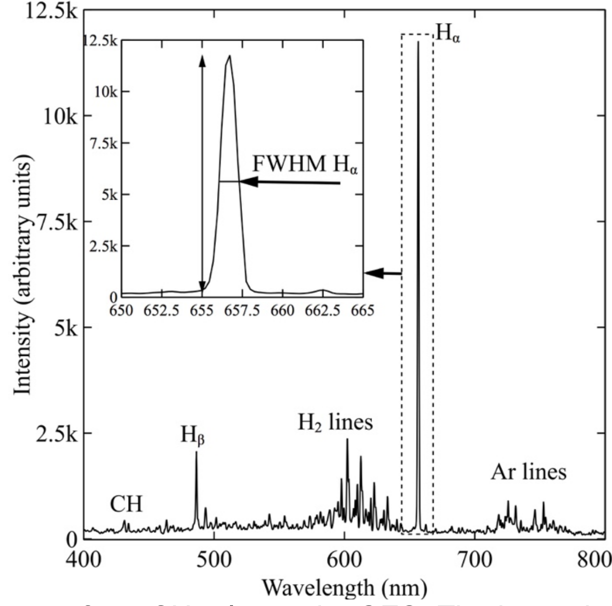

Figure 3. A captured spectrum from CH_4 plasma by OES. The inset shows an example of FWHM measurement of Hα line extracted from spectroscopy results.

2.4.1 Spectral line shape

Spectral line profiles bring energetic information from plasma environment. The width of each line is a result of photon frequency shift because of different broadening mechanisms [41]. Therefore, they can be used as a representative of plasma conditions in further statistical analyses. In this research the FWHM of the H_α line, which is the most apparent feature in the spectra, was employed. An example of the calculation of the H_α line FWHM is presented in the inset of Figure 3.

2.4.2 Actinometry measurements

The intensity of a plasma species emission spectral line is related to both its population in the excited state and its spontaneous emission probability. Moreover, the excited state density is usually 10^{-4} times less than its population in the ground state, which plays major roles in plasma and plasma-surface chemistry [42]. Therefore, emission spectral line intensities may not be employed directly as a measure of plasma species concentration. Actinometry, first introduced by Coburn in 1980 [43], is a technique that enables to estimate the relative densities of a plasma species in the ground state using OES measurements. It helps to measure each species total concentration based on the concentration of a noble gas, known as the actinometer.

In actinometry experiments, a small amount of an inert gas (here argon), which has a similar excitation energy level to that of the probed species (here atomic hydrogen and CH), is used as a reference. The relative concentration of a probed species in the ground state over the actinometer concentration is proportional to their relative spectral line intensity, as described in Eq. (6).

$$\frac{[x]}{Act} = k_x \frac{I_x}{I_{Act}} \quad (6)$$

where [x] and [Act] are the concentrations of x species and the actinometer in their ground state, I_x/I_{ACT} is their ratio of emission intensities, and k_x is a constant value for the given plasma parameters.

However, the proper use of actinometry requires meeting some critical assumptions. First, the two species must be excited from the ground state via a single electron impact excitation. Second both species must have similar energy threshold for excitation. Finally, the predominant de-excitation process should proceed through radiative relaxation, which is the case in our low-pressure plasma.

Actinometry has been previously employed for carbon-containing plasma processes [42,44]. In the present work, a known amount of Ar was used to perform actinometry measurements. The intensity of CH, H_α and H_β emission lines (frequently used in the literature [17,42]) relative to that of Ar at different plasma conditions, were employed to probe their concentration in the plasma environment. The Ar 4p→4s transition (at 750nm) was employed to satisfy the aforementioned criteria of similar energy threshold for excitation [17,42]. Indeed, the etching procedure was always done by using an identical amount of Argon. Therefore, it was possible to use the argon line to estimate some species concentration from actinometry measurements. In this research, the I_x/I_{ACT} ratio was simply employed to probe the species concentrations without applying the related constant (k), as this ratio carries the information related to the concentration variation inside the plasma.

2.5 Statistical analysis – PLSR

The process parameters and OES data were used to build-up the X matrix while DLC structural and mechanical properties allowed to construct the Y matrix. Multivariate analysis of this research is carried out by ProMV© - 15.02 (ProSensus Multivariate) software. Before applying the PLSR model, the raw data were first auto-scaled to normalize the units and the range of variables.

3 RESULTS AND DISCUSSION

Table 2 presents the measured properties of the deposited DLC coatings (D-parameters, internal compressive stresses and deposition rate) and the extracted data from OES (including species concentration index and FWHM of Hα line) at different deposition conditions.

The deposition conditions A and B, which both have a high level of power and bias voltage (Table 2) did not result in any DLC coating at the end of the process, likely because CH_x deposition and hydrogen etching are both involved in a DLC film growth in a competitive manner [45]. The greater population of H atoms observed in A and B conditions (Table 2) resulting from high plasma power along with their high-energy level, because of high bias voltage, confirms the idea that etching rate surpasses the deposition rate in these two sets of observations.

3.1 OES as a process-monitoring tool

Different PLSR models were considered in order to evaluate the OES potential for the prediction of DLC film properties. The first model considers OES and plasma experimental parameters as independent variables (X) that determine DLC properties (Y). The second model only employs the experimental parameters as X to find out how a model without OES data can fit the data. In the third model, the X matrix is only based on OES results. Finally, in the fourth model, the X matrix was built-up using the bias voltage and the OES data (Table 3).

The R^2 value of a model shows how well each model fits its data space. Each new principal component increases the R^2 value but not necessarily the prediction power of the model. A cross-validation method is therefore utilized to determine the number of principal components (A). The Q^2 parameter describes the effect of a new component in a model by evaluating how well it predicts the observations. A model is considered as a good explanation of the data space when the total $Q^2 \geq 0.5$ [46].

Table 3. composition of the X matrix used in the PLS model and their R^2 and Q^2 values.

Model no.	Predictor Matrix		Predicted Matrix	R^2	Q^2	A
	Process	OES				
1	P, M, p, V_b	[CH], [H], $FWHM_{H\alpha}$	DLC properties	0.87	0.7	4
2	P, M, p, V_b	-	DLC properties	0.86	0.7	3
3	-	[CH], [H], $FWHM_{H\alpha}$	DLC properties	0.60	0.2	4
4	V_b	[CH], [H], $FWHM_{H\alpha}$	DLC properties	0.88	0.7	4

As could be intuitively expected, building-up the X matrix with all available input parameters (model 1) lead to a statistically reasonable predictive model with R^2 and Q^2 values of 0.87 and 0.7, respectively. Also evident from Table 3, removing the OES data from the model (model 2) does not lead to a significant decrease of its accuracy as only slight decrease of the R2 value is observed. On the contrary, keeping only OES data (model 3) makes any prediction impossible since both the R^2 and Q^2 values severely decrease. In these circumstances, any prognostic about the DLC properties could not be better than random. This shows that this combination of OES data does not carry enough information about the process to be able to be used alone for DLC properties prediction. This is probably due to the fact that the OES measurement was made on the whole plasma while the effect of the bias voltage is felt only at the vicinity of the sample. Accordingly, it is likely that performing a spatially-resolved OES experiment at the vicinity of the surface sample would have allowed to get better correlation between OES data and DLC properties. In these circumstances, a fourth model (model 4) was developed based on V_b and OES data as the predictor matrix. In this case both the R^2 and the Q^2 values are almost identical to those of model 1. This means that it is possible to replace most of the plasma process parameters (power, duty cycle and pressure) by OES data without impeding the accuracy of the prediction on the DLC properties. The loading plot based on the first two principal components of model 4 is presented in Figure 4. It shows the correlation between the predictive matrix and the response matrix. Variables located in the same quadrant are directly correlated, while those of the opposite quadrants are inversely correlated.

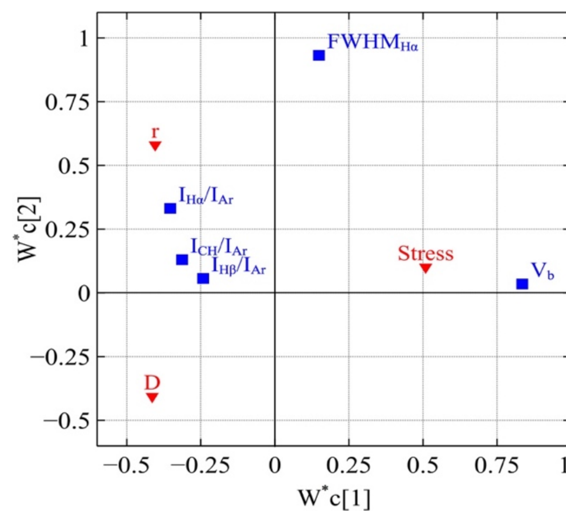

Figure 4: Loading-plot based on first the two principal components (X and Y axis, respectively) of model 4 that shows the structure between predictive (process parameters and OES data) and response variables (coating properties).

To find the most relevant variables that affect the process, one may study the variable importance on the projection (VIPs) produced in a PLSR analysis. The VIP for models 2 and 4 is presented in Figure 5. Parameters with a VIP value higher than unity are considered very important, the values between 0.8 and 1 are considered moderately important, while those lesser than 0.8 are not important in modeling the observations in each specific model. As may be seen in Figure 5-a, the bias voltage (V_b) and plasma power (P) are the two most important parameters, which define energy and type of active plasma species, respectively.

The results presented in Figure 5-b also highlight the importance of the bias voltage to control the DLC layer characteristics. It also shows that the atomic hydrogen and CH radical concentration (as measured by actinometry) also determine to a significant level the properties of DLC. The low importance of FWHMHα (that is frequently used as a measure of gas temperature [47,48]) on the DLC properties is probably related to the fact that the PECVD is a low temperature plasma process that is governed by electron impact dissociation rather than thermal dissociation [49].

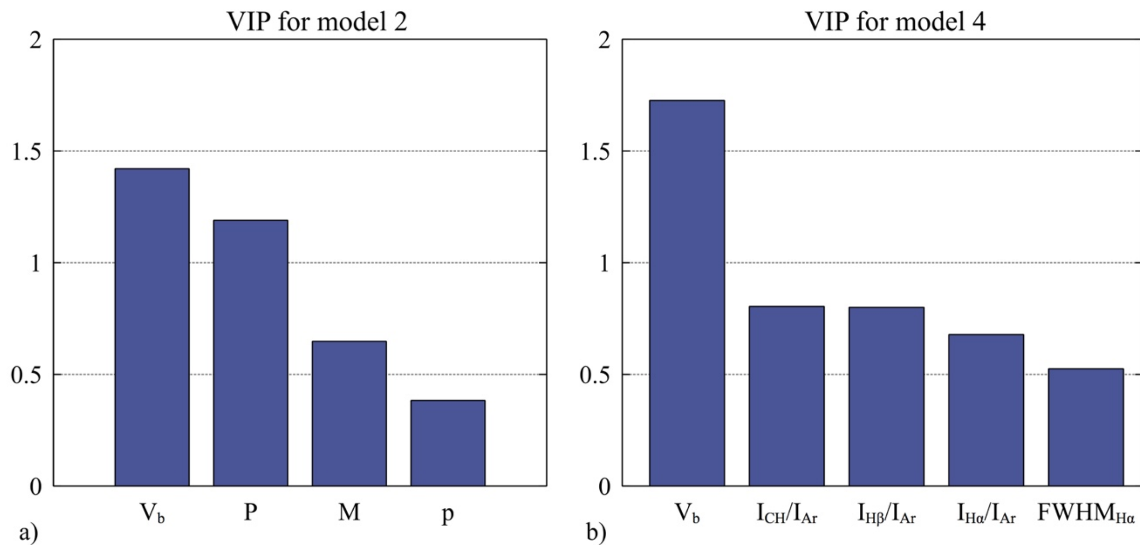

Figure 5. VIP of model 2 and 4. The parameters with a VIP value higher than 1 are very important in the model.

The VIP graph of model 4 introduces the bias voltage as the most important parameter, in agreement with the nature of DLC film formation in which the energy of the incident ions, provided by applying a bias voltage, is responsible for the sp3/sp2 ratio[50]. That said, it is interesting to note that the atomic hydrogen and CH radical concentrations also drive the DLC properties. This latter mathematical observation finds its physical significance because a DLC film formation is an outcome of carbon deposition and hydrogen etching [45].

To understand how DLC properties are affected by each parameter, one needs to study the regression coefficients of the model 4. The coefficients related to film stress, D-parameter (D) and deposition rate (r) that are derived from model 4, are presented in Fig. 6.

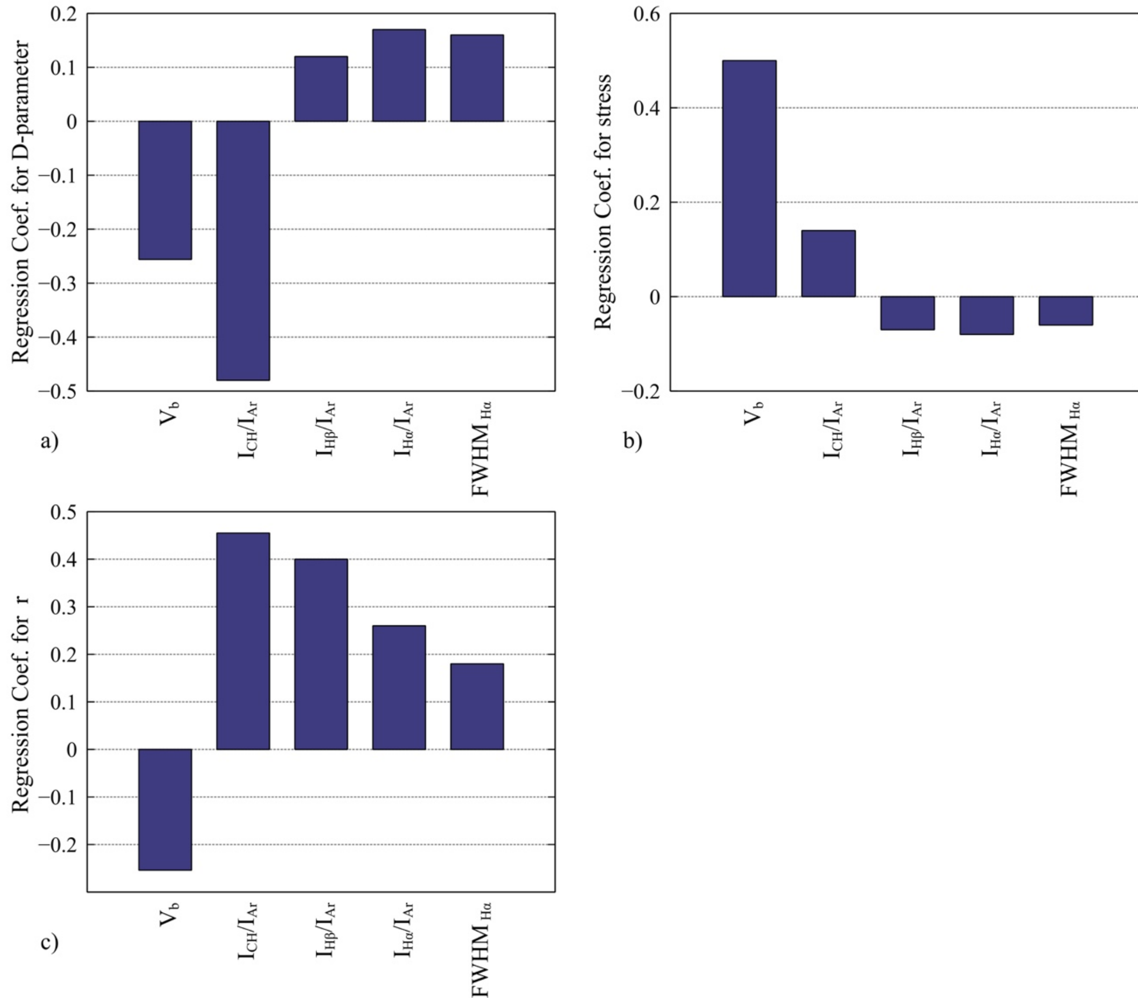

Figure 6. Regression coefficients for a) D-parameter, b) stress, and c) deposition rate of DLC coatings.

As may be seen, the D-parameter is negatively correlated with the bias voltage (V_b) and [CH]. In other words, lower D values, indicative of higher sp^3/sp^2 ratios, are achieved at a higher concentration of CH and larger bias voltage. According to the regression coefficients, the most important parameter for film stress is the bias voltage, (Figure 6-b) which confirms previous results on the effect of bias voltage on the energy of incident ions and consequently, on film stress [51].

Figure 6 also shows that the deposition rate decreases by increasing V_b, probably because of higher etching rate at a higher bias voltage. This figure also evidences the fact that the deposition rate increases with CH radical and atomic H concentration in the plasma at least at low bias (

Figure 6-c). It is likely that the presence of hydrogen in PECVD facilitates DLC growth and, therefore, its deposition rate via different mechanisms that take place either in plasma medium or at the surface/sub-surface of a coating. It helps to break large molecules and prevent the formation of aromatic species that could result in non-diamond coating [52]. Creating active sites via breaking C=C bonds or hydrogen abstraction, and removing soft graphitic or polymeric structures much faster than diamond structure [53–55], are some of the hydrogen roles in DLC film formation that could affect DLC deposition rate (r).

The results presented above led to examine the power of model 4 in predicting new DLC film properties. Therefore, the prediction set of data (Table 2) was employed to evaluate the model. The three graphs in Figure 7 show observed and predicted values for each DLC parameter. Both film

stress and D-parameter have a root-mean-squared (RMS) error value of less than one, which shows a low level of error in prediction. The larger RMS error for deposition rate could be related to the other variables that are not included in this model, such as substrate temperature, as proposed by others [50,56]. However, the prediction curve follows the trend of the observation in all three graphs, therefore confirming the PLSR model potential to predict DLC properties.

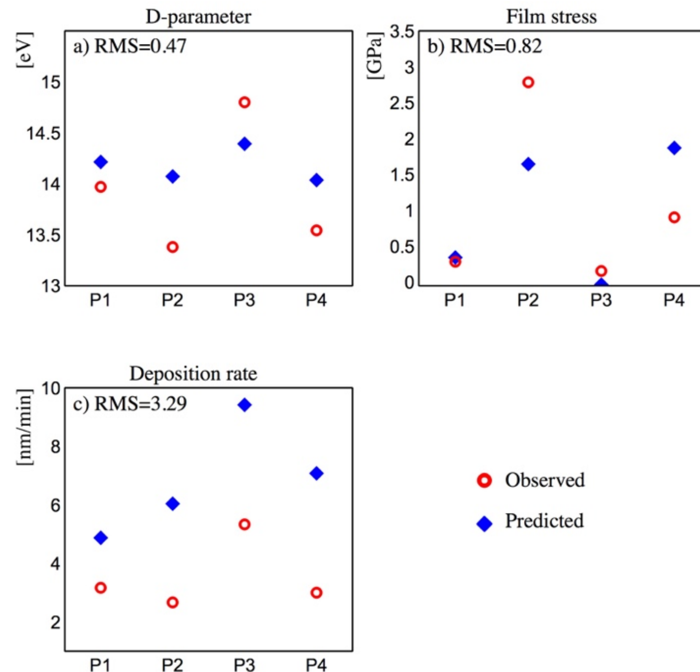

Figure 7. Predicted versus observed values for a) D-parameter, b) DLC stress level, and c) deposition rate.

These findings indicate that PLSR analysis may be used to design a deposition process and to define a process window, based on the predictive power of the model, to achieve a desirable property in the coating. The contour plots in Figure 8 (derived from model 2) shows how DLC stress, D-parameter value and deposition rate (r) change with major process parameters, which are bias voltage (V_b) and plasma power (P). It helps to find the optimum combination of process parameters to achieve a desired film structure and properties. That could also be employed to design a graded DLC structure to reduce the risk of film delamination due to high internal compressive stress. In this way, an option is to start depositing a coating with moderate stress and medium D-parameter (Figure 8-a) for less stress at the interface and change it gradually toward a high stress and lower–D parameter coating (Figure 8-b), which also has more diamond like properties. Figure 8-c roughly depicts the previous starting and the end point windows superimposed on the deposition rate contour plot. It helps to choose a deposition system with higher deposition rate.

At this point, one could question the influence of individual measurement uncertainties on the overall PLSR model. In fact, only few publications investigated this particular issue. In a very interesting study, Wolthuis et al. estimated the influence of experimental parameters on the prediction error of PLS calibration models based on Raman spectra. Basically, they concluded that it is very difficult to assess the propagation of the different errors in the total prediction error. Accordingly, they suggested to use a systematic approach, based on simulation and measurements of a simple two-component system to identify and prioritize possible improvements in both hardware and experimental protocols, therefore leading to a possible improvement of the accuracy and robustness of more complex multi-component models.

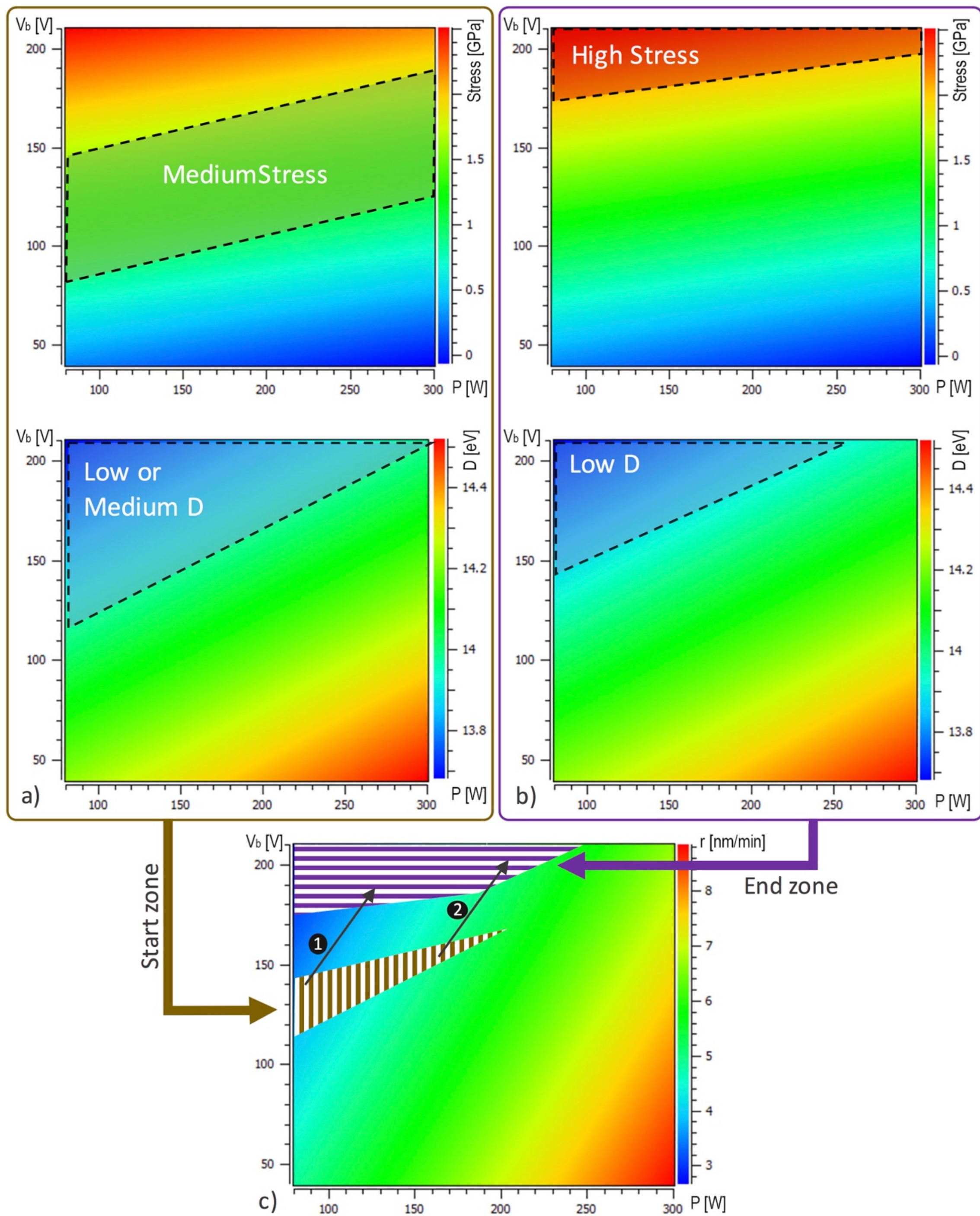

Figure 8. A graded DLC coating (more adhesive to substrate and hard structure at the top layers) can be designed using contour plots derived from model 2, based on bias voltage and plasma power. At the very first layers of the coating (starting zone) a combination of Medium stress and medium to low D value is required (a), while high stress and low D value are preferred for the outermost layers (b). c) contour plot of deposition rate with starting and ending zones then can be employed to select a proper deposition rate ((1): lower rate, (2): higher rate).

4 CONCLUSIONS

A PLSR method, which is a multivariate statistical analysis method, was employed to compare two PECVD control process protocols. On one hand, the first protocol took the advantage of using plasma experimental parameters such as bias voltage, plasma duty cycle, plasma pressure, and power used to generate the discharge. On the other hand, the second process control was based on using parameters derived from optical emission spectroscopy. Although it was demonstrated that the bias voltage value has to be kept in any model aiming at controlling DLC coating process, it was also found that all other aforementioned plasma parameters could be advantageously replaced by optical emission spectroscopy data, therefore allowing to reproduce DLC properties in any plasma reactor configuration. This paves the way to use OES as a monitoring tool for DLC deposition process, especially in multilayer or gradient DLC film deposition, where in situ film properties have to be modified during the deposition process.

ACKNOWLEDGEMENTS

The authors would like to thank Dr. Ranna Tolouei and Dr. Pascal Chevallier for their scientific supports. This work was partially supported by NSERC-Canada and FRQNT (Quebec).

REFERENCES

[1] J.C. Angus, Diamond and diamond-like phases - Extended Abstract, Diam. Relat. Mater. 1 (1991) 61–62.
[2] J. Robertson, The deposition mechanism of diamond-like a-C and a-C:H, Diam. Relat. Mater. 3 (1994) 361–368.
[3] Y. Lifshitz, Diamond-like carbon — present status, Diam. Relat. Mater. 8 (1999) 1659–1676.
[4] T.A. Friedmann, J.P. Sullivan, J.A. Knapp, D.R. Tallant, D.M. Follstaedt, D.L. Medlin, P.B. Mirkarimi, Thick stress-free amorphous-tetrahedral carbon films with hardness near that of diamond, Appl. Phys. Lett. 71 (1997) 3820.
[5] S. Takabayashi, K. Okamoto, H. Sakaue, T. Takahagi, K. Shimada, T. Nakatani, Annealing effect on the chemical structure of diamondlike carbon, J. Appl. Phys. 104 (2008) 43512.
[6] H.W. Choi, J.-H. Choi, K.-R. Lee, J.-P. Ahn, K.H. Oh, Structure and mechanical properties of Ag-incorporated DLC films prepared by a hybrid ion beam deposition system, Thin Solid Films. 516 (2007) 248–251.
[7] J.L. Endrino, R. Escobar Galindo, H.-S. Zhang, M. Allen, R. Gago, A. Espinosa, A. Anders, Structure and properties of silver-containing a-C(H) films deposited by plasma immersion ion implantation, Surf. Coatings Technol. 202 (2008) 3675–3682.
[8] N.M. Chekan, N.M. Beliauski, V.V. Akulich, L.V. Pozdniak, E.K. Sergeeva, A.N. Chernov, V.V. Kazbanov, V. a. Kulchitsky, Biological activity of silver-doped DLC films, Diam. Relat. Mater. 18 (2009) 1006–1009.
[9] J. Meneve, E. Dekempeneer, W. Wegener, J. Smeets, Low friction and wear resistant a-C:H/a-Si1−xCx:H multilayer coatings, Surf. Coatings Technol. 86–87 (1996) 617–621.
[10] S. Logothetidis, C.A. Charitidis, M. Gioti, Y. Panayiotatos, Comprehensive study on the properties of multilayered amorphous carbon films, Diam. Relat. Mater. 9 (2000) 756–760.
[11] Z. Xu, Y.J. Zheng, F. Jiang, Y.X. Leng, H. Sun, N. Huang, The microstructure and mechanical properties of multilayer diamond-like carbon films with different modulation ratios, Appl. Surf. Sci. 264 (2013) 207–212.
[12] T.M. Chao, A.H. Tan, DLC deposition parameters optimization for head disk design interface with a thermal protrusion slider from tribological point of view, Mater. Des. 48 (2013) 58–67.

[13] H. Ronkainen, J. Koskinen, S. Varjus, K. Holmberg, Experimental design and modelling in the investigation of process parameter effects on the tribological and mechanical properties of r.f.-plasma-deposited a-C:H films, Surf. Coatings Technol. 122 (1999) 150–160.
[14] C. Corbella, M. Vives, G. Oncins, C. Canal, J.L. Andújar, E. Bertran, Characterization of DLC films obtained at room temperature by pulsed-dc PECVD, Diam. Relat. Mater. 13 (2004) 1494–1499.
[15] V.A. Godyak, Measuring EEDF in Gas Discharge Plasmas, in: Plasma-Surface Interact. Process. Mater., Springer Netherlands, 1990: pp. 95–134.
[16] J.R. Woodworth, M.E. Riley, D.C. Meister, B.P. Aragon, M.S. Le, H.H. Sawin, Ion energy and angular distributions in inductively coupled radio frequency discharges in argon, J. Appl. Phys. 80 (1996) 1304.
[17] A. Pastol, Y. Catherine, Optical emission spectroscopy for diagnostic and monitoring of CH , plasmas used for a-C : H deposition, J. Phys. D. 23 (1990) 799–805.
[18] V. Schulz-von Der Gathen, Diagnostic studies of species concentrations in a capacitively coupled RF plasma containing CH4 – H2 – Ar, Plasma Sources Sci. Technol. 10 (2001) 530.
[19] G. Lombardi, K. Hassouni, F. Bénédic, F. Mohasseb, J. Röpcke, A. Gicquel, Spectroscopic diagnostics and modeling of Ar/H2/CH4 microwave discharges used for nanocrystalline diamond deposition, J. Appl. Phys. 96 (2004) 6739.
[20] S. Naito, H. Nomura, T. Goto, Measurement of CH3 Radical in RF Methane:Rare Gas Plasma Using Infrared Diode Laser Absorption Spectroscopy, LASER Eng. 20 (1992) 746.
[21] N. Mutsukura, Deposition of Diamondlike Carbon Film and Mass Spectrometry Measurement in CH 4 / N 2 RF Plasma, Plasma Chem. Plasma Process. 21 (2001) 265–277.
[22] a. Soum-Glaude, L. Thomas, A. Dollet, P. Ségur, M.C. Bordage, Argon/tetramethysilane PECVD: From process diagnostic and modeling to a-Si:C:H hard coating composition, Diam. Relat. Mater. 16 (2007) 1259–1263.
[23] H. Zhou, J. Watanabe, M. Miyake, A. Ogino, M. Nagatsu, R. Zhan, Optical and mass spectroscopy measurements of Ar/CH4/H2 microwave plasma for nano-crystalline diamond film deposition, Diam. Relat. Mater. 16 (2007) 675–678.
[24] I. Hutchinson, Principles of Plasma Diagnostics, Cambridge: Cambridge Universty Press, 2002.
[25] M. Mavadat, A. Ricard, C. Sarra-Bournet, G. Laroche, Determination of ro-vibrational excitations of N 2 (B , v ′) and N 2 (C , v ′) states in N 2 microwave discharges using visible and IR spectroscopy, J. Phys. D. Appl. Phys. 44 (2011) 155207.
[26] S. Wold, M. Sjostrom, PLS-regression : a basic tool of chemometrics, Chemom. Intell. Lab. Syst. 58 (2001) 109–130.
[27] G.E.P. Box, S. Hunter, J, W.G. Hunter, Statistics for experimenters, Design, Innovation and Discovery, 2nd ed., Wiley interscience, 2005.
[28] G.G. Stoney, The tension of metallic films deposited by electrolysis, Proc. R. Soc. London. Ser. A, Contain. Pap. a Math. Phys. Character. 82 (1909) 172–175.
[29] A.A. Galuska, H.H. Madden, Electron spectroscopy and amorphous carbon, Appl. Surf. Sci. 32 (1988) 253–272.
[30] T. Sharda, High resolution Auger electron spectroscopy studies on (100) and (111) facets of chemical vapor deposited diamond, J. Vac. Sci. Technol. A Vacuum, Surfaces, Film. 16 (1998) 413.
[31] Y. Mizokawa, T. Miyasato, K.M. Geib, Comparison of the C KLL first-derivative Auger spectra from XPS and AES using diamond, graphite, SiC and diamond like carbon films, Surf. Sci. 182 (1987) 431–438.
[32] J.C. Lascovitch, R. Giorgi, S. Scaglione, Evaluation of the sp2 / sp3 ratio in amorphous and XAES carbon structure by XPS, Appl. Surf. Sci. 47 (1991) 17–21.
[33] H. Chu, E. Den Hartog, A. Lefkow, J. Jacobs, L. Anderson, M. Lagally, J. Lawler, Measurements of the gas kinetic temperature in a CH4-H2 discharge during the growth of diamond, Phys. Rev. A. 44 (1991) 3796–3803.

[34] K.J. Clay, S.P. Speakman, G.A.J. Amaratunga, S.R.P. Silva, Characterization of a-C:H:N deposition from CH4/N2 rf plasmas using optical emission spectroscopy, J. Appl. Phys. 79 (1996) 7227–7233.
[35] V.M. Polushkin, A.T. Rakhimov, V.A. Samorodov, N.V. Suetin, M. A. Timofeyev, OES study of plasma processes in d.c. discharge during diamond film deposition, Diam. Relat. Mater. 3 (1994) 1385–1388.
[36] G. Zambrano, H. Riascos, P. Prieto, E. Restrepo, A. Devia, C. Rincón, Optical emission spectroscopy study of r.f. magnetron sputtering discharge used for multilayers thin film deposition, Surf. Coatings Technol. 172 (2003) 144–149.
[37] D.M. Gruen, Carbon dimer, C2, as a growth species for diamond films from methane/hydrogen/argon microwave plasmas, J. Vac. Sci. Technol. A Vacuum, Surfaces, Film. 13 (1995) 1628.
[38] C. Wild, Process monitoring of a-C:H plasma deposition, J. Vac. Sci. Technol. A Vacuum, Surfaces, Film. 5 (1987) 2227.
[39] K. Teii, Diagnostics of the diamond depositing inductively coupled plasma by electrostatic probes and optical emission spectroscopy, J. Vac. Sci. Technol. A Vacuum, Surfaces, Film. 17 (1999) 138.
[40] K.W. Hemawan, R.J. Hemley, Optical emission diagnostics of plasmas in chemical vapor deposition of single-crystal diamond, J. Vac. Sci. Technol. A Vacuum, Surfaces, Film. 33 (2015) 61302.
[41] S. Svanberg, Atomic and Molecular Spectroscopy- Basic Aspects and Practical Applications, Springer-Verlag, 1992.
[42] A. Gicquel, M. Chenevier, K. Hassouni, A. Tserepi, M. Dubus, Validation of actinometry for estimating relative hydrogen atom densities and electron energy evolution in plasma assisted diamond deposition reactors, J. Appl. Phys. 83 (1998) 7504.
[43] J.W. Coburn, M. Chen, Optical emission spectroscopy of reactive plasmas: A method for correlating emission intensities to reactive particle density, J. Appl. Phys. 51 (1980) 3134.
[44] T. Lang, J. Stiegler, Y. von Kaenel, E. Blank, Optical emission diagnostics and film growth during microwave-plasma-assisted diamond CVD, Diam. Relat. Mater. 5 (1996) 1171–1184.
[45] A. Poukhovoi, S. Schipporeit, Assessment of spectroscopic methods for the characterisation of DLC films deposited by PECVD, J. Optoelectron. Adv. Mater. 14 (2012) 383–392.
[46] M. Tenenhaus, La régression PLS : théorie et pratique, Éditions Technip, Paris, 1998.
[47] A. Gicquel, K. Hassouni, Y. Breton, M. Chenevier, J.C. Cubertafon, Gas temperature measurements by laser spectroscopic techniques and by optical emission spectroscopy, Diam. Relat. Mater. 5 (1996) 366–372.
[48] M.H. Elghazaly, A.M. Abd Elbaky, A.H. Bassyouni, H. Tuczek, Spectroscopic Studies of Plasma Temperature in a Low-Pressure Hydrogen Plasma, J. Quant. Spectrosc. Radiat. Transf. 61 (1999) 503–507.
[49] A.A. Fridman, L.A. Kennedy, Plasma physics and engineering, 2nd ed, CRC Press, Boca Raton, FL, 2011.
[50] J. Robertson, Diamond-like amorphous carbon-Review, Mater. Sci. Eng. R Reports. 37 (2002) 129–281.
[51] M.M.M. Bilek, D.R. McKenzie, A comprehensive model of stress generation and relief processes in thin films deposited with energetic ions, Surf. Coatings Technol. 200 (2006) 4345–4354.
[52] M. Frenklach, The role of hydrogen in vapor deposition of diamond, J. Appl. Phys. 65 (1989) 5142.
[53] L. Schäfer, C.-P. Klages, U. Meier, K. Kohse-Höinghaus, Atomic hydrogen concentration profiles at filaments used for chemical vapor deposition of diamond, Appl. Phys. Lett. 58 (1991) 571.
[54] N. Setaka, Diamond synthesis from vapor phase and its growth process, J. Mater. Res. 4 (1989) 664–670.

[55] B.D. Thoms, P.E. Pehrsson, J.E. Butler, A vibrational study of the adsorption and desorption of hydrogen on polycrystalline diamond, J. Appl. Phys. 75 (1994) 1804–1810.
[56] Y. Lifshitz, Hydrogen-free amorphous carbon films : correlation between growth conditions and properties, Diam. Relat. Mater. 5 (1996) 388–400.
[57] M. Shimozuma, G. Tochitani, H. Tagashira, Optical emission diagnostics of H2+CH4 50-Hz–13.56-MHz plasmas for chemical vapor deposition, J. Appl. Phys. 70 (1991) 645.
[58] R. Wolthuis, G.C.H. Tjiang, G.J. Puppels, T.C. Bakker Schut. Estimating the influence of experimental parameters on the prediction error of PLS calibration models based on Raman spectra, J. Raman Spectrosc. 37 (2006) 447.